Magnetic Nano-skyrmion Lattice Observed in a Si-Wafer-Based Multilayer System

Anika Schlenhoff,*,† Philipp Lindner,† Johannes Friedlein,† Stefan Krause,† Roland Wiesendanger,† Michael Weinl,‡ Matthias Schreck,‡ and Manfred Albrecht‡

†Department of Physics, University of Hamburg, Jungiusstraße 11, 20355 Hamburg, Germany and ‡Institute of Physics, University of Augsburg, Universitätsstraße 1, 86135 Augsburg, Germany

ABSTRACT Growth, electronic properties, and magnetic properties of an Fe monolayer (ML) on an Ir/YSZ/Si(111) multilayer system have been studied using spin-polarized scanning tunneling microscopy. Our experiments reveal a magnetic nano-skyrmion lattice, which is fully equivalent to the magnetic ground state that has previously been observed for the Fe ML on Ir(111) bulk single crystals. In addition, the experiments indicate that the interface-stabilized skyrmion lattice is robust against local atomic lattice distortions induced by multilayer preparation.

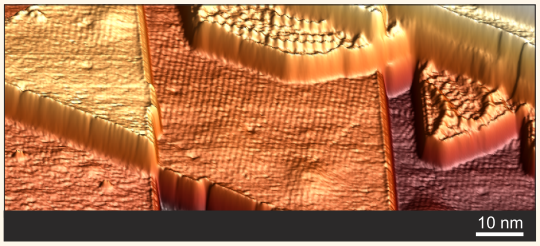

KEYWORDS: spintronics · skyrmions · SP-STM · multilayer systems · silicon wafer

Magnetic skyrmions are localized spin configurations with a whirling configuration.[1,2] They are extremely well defined given that they always occur with a specific rotational sense. In addition, they are topologically stable: they cannot be deformed to a ferromagnetic or other magnetic state without overcoming an energy barrier. Due to this robustness, these particle-like skyrmions offer new exciting possibilities for spintronic applications, using them as carriers of digital information.[3,4] Recently, an atomic-scale two-dimensional magnetic skyrmion lattice that is stabilized by Dzyaloshinskii–Moriya interactions at the Fe/Ir(111) interface has been discovered using spin-polarized scanning tunneling microscopy (SP-STM).[5] The selective writing and deleting of individual nano-skyrmions by injecting a spin-polarized tunneling current into a bilayer metal system has already been demonstrated.[6] It was also reported that very low current densities are sufficient to move a skyrmion, compared to the current-induced movement of a domain wall.[7,8]

Up to now, interface-stabilized nano-skyrmion lattices in metal films have been studied only on metallic bulk single-crystal substrates.[5,6,9,10] Similar to the Si-based technology of today, an important prerequisite for future skyrmion-based spintronic applications is the mass production of skyrmionic devices using multilayer growth. In past years, heteroepitaxial growth of Ir on Si(111) with an yttria-stabilized zirconia (YSZ) buffer layer has been developed.[11,12] Using Si wafers as substrates, this technique can be easily implemented into standard Si-based fabrication. Ir/YSZ/Si(111) wafers of up to 4 in. in diameter have already been prepared and characterized, revealing basically twin-free heteroepitaxial Ir(111) films on the YSZ/Si(111) support with low mosaic spread ($\leq$0.2°).[12,13]

In our study, we epitaxially grow Fe onto the Ir/YSZ/Si(111) surface and test the system for a magnetic nano-skyrmion lattice. After we deposited nominally 0.8 atomic layer (AL) of Fe on the substrate, the sample was inserted into the microscope and cooled to our measurement temperature of 26.4 K.

RESULTS AND DISCUSSION

A topography overview of a typical sample is shown in Figure 1a. A small ac modulation voltage (U_{mod} = 40 mV, f = 4.333 kHz) was added to the applied sample bias voltage U in order to record the spatially resolved differential tunneling conductance, dI/dU, by a lock-in technique simultaneously to the constant-current topography image. The topography is overlaid with the dI/dU

* Address correspondence to aschlenh@physnet.uni-hamburg.de.

Received for review January 22, 2015 and accepted May 6, 2015.

Published online May 12, 2015
10.1021/acsnano.5b01146

© 2015 American Chemical Society

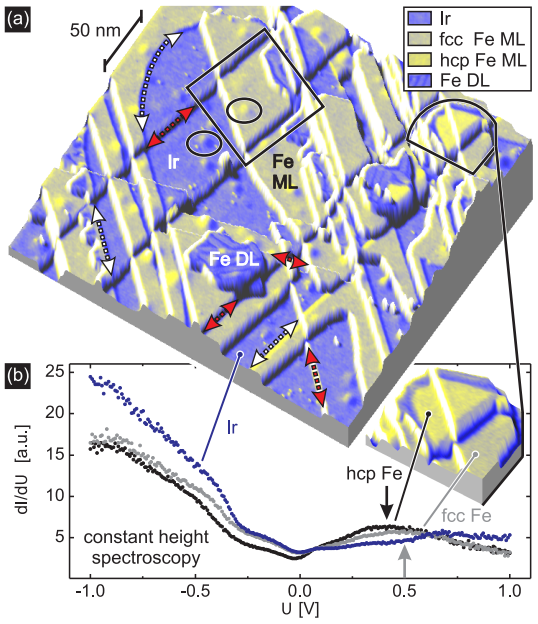

Figure 1. (a) Topography of 0.8 AL Fe on Ir/YSZ/Si(111) overlaid with the simultaneously recorded d*I*/d*U* signal (*U* = 260 mV, *I* = 1 nA). The Fe ML grows at the intrinsic step edges and the slip lines of the Ir surface (white arrows). Small Fe DL islands are visible. Slip lines that evolve when cooling the system for the experiments break up the already-grown Fe film (red arrows). Defects resulting from sputtering of the substrate are visible on Ir and Fe (encircled). (b) Constant-height spectroscopy above Ir and hcp and fcc Fe ML (stabilization parameters: *I* = 1 nA, *U* = 1 V). A typical peak at *U* ≈ +350 mV is visible for the hcp stacking, whereas it is located at *U* ≈ +500 mV for the fcc stacking (positions marked by arrows). Inset: Closer view of the area marked in (a) showing both types of ML areas.

signal in Figure 1a. Regions of monolayer (ML) coverages coexist with regions of the bare Ir surface. The d*I*/d*U* signal reveals an electronic contrast between them. Small double-layer (DL) areas are also present. While the Fe ML appears flat, the Fe DL shows a reconstruction due to strain relaxation.[14]

The Fe grows mainly at the step edges of the Ir surface, as it is also known from the step-flow growth mode on the Ir(111) bulk single crystal.[14,15] Beside an intrinsic curved step at the top of the image, straight steps running along the main crystallographic directions can be observed, which are characteristic for the underlying Ir/YSZ/Si(111) surface.[16] These steps of atomic height are slip lines that result from gliding processes or dislocation movements in the Ir film occurring during the thermal treatment of the Ir/YSZ/Si(111) substrate. They arise due to the different thermal expansion coefficients of the individual components of the Ir/YSZ/Si(111) multilayer system. The directions of the slip lines reflect the hexagonal sample symmetry. Since the Fe grows at all of these step edges, they lead to multiple growth directions of the Fe film. Likewise, additional slip lines evolve when cooling to low temperature for the SP-STM experiments, resulting in multiple breakups of the Fe ML and DL patches, as is observed in Figure 1a.

On the Ir surface, as well as on the Fe ML, shallow protrusions are visible. These defects that have been found on the bare substrate before originate from sputtering during sample preparation.[16] They are most likely caused by Ar^+ ions incorporated into the Ir film. For Ir(111) single crystals, these volume defects can be removed by flash annealing after sputtering at temperatures between 1350 and 1800 K.[10,15] In the case of Ir/YSZ/Si(111), temperatures above ~1300 K cannot be applied because they result in a dewetting of the metal film.[16]

Besides the electronic contrast between Fe and Ir, the signal of the differential tunneling conductance, d*I*/d*U*, in Figure 1a reveals two different types of Fe ML areas. A closer view of an area that exhibits both types of ML patches is shown in the inset of Figure 1b. For Fe/Ir(111), it is known that the ML grows in two different in-plane commensurate stackings, face-centered cubic (fcc) and hexagonal close-packed (hcp).[14,15] They can be distinguished by their different electronic structure. In Figure 1b, constant-height d*I*/d*U* spectroscopy curves, taken on the Ir/YSZ/Si(111) surface and the two different types of Fe ML areas, are shown. For both types of ML areas, a broad empty-state peak at positive sample bias voltage is observed. The predominant type exhibits a peak at *U* ≈ +500 mV, which is typical for the fcc stacking, as has been observed in experimental spectra for Fe on Ir(111).[14] For the scarce ML patches, the peak is shifted to *U* ≈ +350 mV, which is also consistent with experimental spectra taken on hcp-stacked Fe on the Ir(111) single crystal.[14] We conclude that the bright Fe ML patches in Figure 1a grow in hcp stacking, whereas all of the other areas of ML coverage exhibit an fcc stacking. The preference of the fcc-stacked regions results from the high density of slip lines where Fe continues the arrangement of the Ir atoms and therefore grows in fcc stacking. Summing up, our measurements show that the electronic properties of a submonolayer coverage of Fe on Ir/YSZ/Si(111) are equivalent to those on the (111) surface of Ir bulk single crystals, despite substantial variations in surface topography induced by sample preparation.

The observed electronic equivalence raises the question about the magnetic properties of the Fe/Ir/YSZ/Si(111) multilayer system in comparison to the topographically much simpler Fe/Ir(111) bulk single-crystal system. A closer view of the area marked in Figure 1a is shown in Figure 2a. The constant-current SP-STM image shows an extended fcc-stacked Fe ML film that is broken by two slip lines running from the bottom to the top of the image. At the top of the image, an Fe DL region with its reconstruction is observable. It is broken by a slip line that runs, in this case, horizontally through the image. At the bottom, a small region of the bare Ir surface is visible. On the Fe ML, a regular superstructure is observed. In SP-STM, the spin-polarized tunneling current depends on the relative

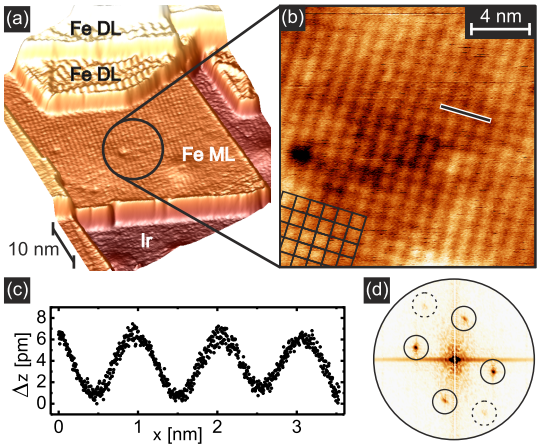

Figure 2. (a) Constant-current SP-STM image of the sample area marked in Figure 1a. (b) Closer view of the fcc Fe ML area marked in (a). A square lattice is visible. The inset shows a schematic. (c) Line profile along the direction indicated in (b). (d) Fourier transform of (b). Black circles mark the contribution from the magnetic unit cell, and dashed circles the spots caused by the TAMR effect (U = 10 mV, I = 4 nA, T = 26.4 K).

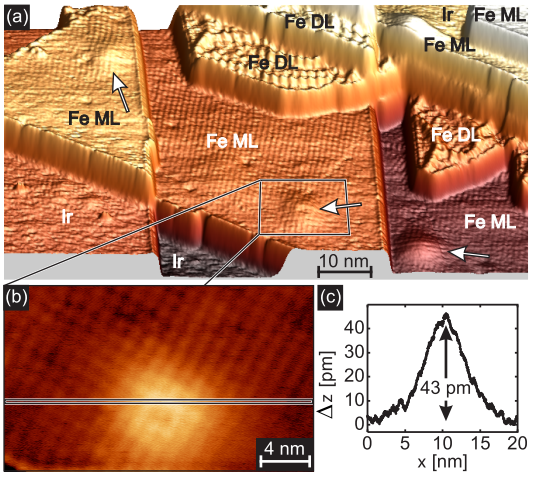

Figure 3. (a) Constant-current SP-STM image of the sample around the area shown in Figure 2a. On the Fe ML, sputtering defects are visible (marked by arrows). (b) Closer view of the area marked in (a). Also on the sputtering defect, the square lattice is visible. (c) Line profile along the direction indicated in (b). The maximum height of the defect is ≈43 pm (U = 10 mV, I = 4 nA, T = 26.4 K).

orientation between the tip and the local sample magnetization.[17] Consequently, the variation of the tip−sample distance in constant-current SP-STM experiments on an electronically homogeneous system reflects the magnetic structure of the surface. In Figure 2b, a zoomed-in image on the Fe ML is shown. It reveals a square lattice symmetry of the superstructure. The line profile in Figure 2c taken along the direction indicated in (b) reveals a periodicity of about 1 nm and a corrugation of about 6 pm. Figure 2d shows the Fourier transform (FT) of the SP-STM data of Figure 2b, revealing six distinct spots. The spots marked with black circles correspond to the square lattice shown in the inset of Figure 2b, with an observed angle between the lattice vectors $\theta = 91 \pm 3°$ and a lattice constant of 1.02 ± 0.08 nm. The observed square lattice resembles the magnetic contrast that has been found for the Fe ML on Ir(111) single crystals.[5,9,10] It can be assigned to a skyrmion lattice that is stabilized at the interface between Fe and Ir(111). The corresponding magnetic unit cell is known to have a a size of approximately 1×1 nm^2 and consists of about 15 atoms. Both the observed angle between the lattice vectors and the lattice constant reproduce well the experimental findings on the Ir(111) bulk single crystal.[5,9,10] Note that the measured corrugation along the horizontal direction is stronger than that along the vertical direction in our experiment, which is attributed to a canted tip magnetization.[18] In the FT shown in Figure 2d, this results in a variation of the magnetic contrast spot intensities. The FT spots marked in the dashed circles indicate a periodicity that is reduced by a factor of $\sqrt{2}$ compared to the magnetic unit cell. They are attributed to the tunneling anisotropic magnetoresistance (TAMR) effect that can be observed at low bias voltages.[5,19,20] In summary, our experiments demonstrate that the magnetic ground state of the Fe ML on an Ir/YSZ/Si(111) substrate is identical to that on the (111) surface of Ir bulk single crystals. The magnetic nano-skyrmion lattice of the Fe ML is also observed on a Si-wafer-based multilayer system that is fabricated by industrial preparation techniques.

Zooming out of the sample area of Figure 2a reveals the magnetic square lattice evolving also on the top left and bottom right Fe ML area, as shown in Figure 3a. As mentioned before, they are separated from the middle Fe ML patch by slip lines. On each ML patch, a sputtering defect is visible, causing a local protrusion. Interestingly, the magnetic square lattice is observable even on these local defects. A closer view of the middle ML area with the sputtering defect is shown in Figure 3b. The square unit cell of the superstructure, which resembles the unit cell of the magnetic skyrmion lattice, is clearly visible all over the defect and even on top of it. No distortion of the magnetic skyrmion lattice is observed. The line profile in Figure 3c, taken along the direction indicated in (b), reveals that the defect exhibits a maximum height of $h \approx 43$ pm and is about 8 nm wide. Taking the interatomic distance $a/\sqrt{2}$ with the lattice constant a = 2.22 Å of Ir into account, we determine that the local stress is relieved over approximately 25 atoms in the horizontal direction. Hence, the vertical lattice displacement between next neighbors can be estimated to 1.7 pm, which is about 1% of the distance of the (111) planes in Ir. Obviously, the skyrmion lattice is robust against local atomic lattice distortions induced by structural point defects.

CONCLUSIONS

In summary, our SP-STM experiments at low temperature show that a magnetic nano-skyrmion lattice is formed in the Fe ML on the Ir/YSZ/Si(111) multilayer

system. Despite substantial variations in surface topography, such as volume defects, slip lines, and multiple growth directions induced by multilayer preparation, the electronic and magnetic properties of the Fe ML on the Si-wafer-based substrate are comparable to those that have been observed on the Fe ML on Ir(111) bulk single crystals. Our experimental results pave the way for the use of multilayer substrates in magnetic surface studies by SP-STM that are based so far on single-crystal metal substrates. Being performed on an up-scalable Si-based substrate, our work promotes spintronic applications of nano-skyrmions as carriers of digital information that can be fabricated on a wafer scale by industrial processes that are fully compatible with standard semiconductor technology.

METHODS

The experiments were performed under ultrahigh vacuum (UHV) conditions with a pressure below 1×10^{-8} Pa using a home-built spin-polarized scanning tunneling microscope at variable temperatures. Within our experimental setup, the entire microscope including the tip is cooled to maximize the thermal stability. For the SP-STM experiments, antiferromagnetic bulk Cr tips were used to avoid an undesired dipolar coupling with the sample.[18] All experiments presented in this paper have been performed at a temperature of 26.4 K and in the absence of any external magnetic field. The Ir/YSZ/Si(111) multilayer system was prepared in Augsburg according to a previously described method.[12] A (111)-oriented Si wafer was first covered by a YSZ layer with a thickness of 150 nm by means of pulsed laser deposition from a ZrO_2 target containing 6.5 mol % of $YO_{1.5}$.[21] The YSZ serves as a buffer layer, preventing silicide formation of the metal with the subjacent silicon. In addition, it transfers the epitaxial orientation from the Si single crystal to the metal film. On top of the YSZ layer, a 600 nm thick Ir film was deposited by molecular beam epitaxy. The first 20 nm was grown at a rate of 0.004 nm/s at 920 K. For the remaining 580 nm, the growth rate was increased to 0.02 nm/s and the temperature decreased to 820 K. This procedure guaranteed flat films with high structural perfection, as proven by a polar and azimuthal mosaic spread of 0.089° and 0.075°, respectively. For the present experiments, the high total thickness facilitated repeated sputtering and annealing cycles. However, for future applications, an identical functionality can be achieved with Ir film thicknesses well below 100 nm. The 10×10 mm^2 pieces were cut from the wafers, mounted to sample holders, and introduced into the UHV chamber in Hamburg. The Ir/YSZ/Si(111) substrate was then prepared *in situ* by sputtering with Ar^+ ions at room temperature and annealing under an oxygen atmosphere at 820 K, followed by a high-temperature flash (1060 K). Iron was deposited by molecular beam epitaxy at elevated substrate temperature (450 K).

Conflict of Interest: The authors declare no competing financial interest.

Acknowledgment. We thank A. Sonntag for helpful discussions. Financial support from the DFG *via* SFB 668 is gratefully acknowledged.

REFERENCES AND NOTES

1. Mühlbauer, S.; Binz, B.; Jonietz, F.; Pfleiderer, C.; Rosch, A.; Neubauer, A.; Georgii, R.; Böni, P. Skyrmion Lattice in a Chiral Magnet. *Science* **2009**, *323*, 915–919.
2. Nagaosa, N.; Tokura, Y. Topological Properties and Dynamics of Magnetic Skyrmions. *Nat. Nanotechnol.* **2013**, *8*, 899–911.
3. Fert, A.; Cros, V.; Sampaio, J. Skyrmions on the Track. *Nat. Nanotechnol.* **2013**, *8*, 152–156.
4. Kiselev, N. S.; Bogdanov, A. N.; Schaefer, R.; Rößler, U. K. Chiral Skyrmions in Thin Magnetic Films: New Objects for Magnetic Storage Technologies? *J. Phys. D: Appl. Phys.* **2011**, *44*, 392001–392004.
5. Heinze, S.; von Bergmann, K.; Menzel, M.; Brede, J.; Kubetzka, A.; Wiesendanger, R.; Bihlmayer, G.; Blügel, S. Spontaneous Atomic-Scale Magnetic Skyrmion Lattice in Two Dimensions. *Nat. Phys.* **2011**, *7*, 713–718.
6. Romming, N.; Hanneken, C.; Menzel, M.; Bickel, J. E.; Wolter, B.; von Bergmann, K.; Kubetzka, A.; Wiesendanger, R. Writing and Deleting Single Magnetic Skyrmions. *Science* **2013**, *341*, 636–639.
7. Yu, X.; Kanazawa, N.; Zhang, W.; Nagai, T.; Hara, T.; Kimoto, K.; Matsui, Y.; Onose, Y.; Tokura, Y. Skyrmion Flow near Room Temperature in an Ultralow Current Density. *Nat. Commun.* **2012**, *3*, 988–993.
8. Sampaio, J.; Cros, V.; Rohart, S.; Thiaville, A.; Fert, A. Nucleation, Stability and Current-Induced Motion of Isolated Magnetic Skyrmions in Nanostructures. *Nat. Nanotechnol.* **2013**, *8*, 839–844.
9. von Bergmann, K.; Kubetzka, A.; Pietzsch, O.; Wiesendanger, R. Interface-Induced Chiral Domain Walls, Spin Spirals and Skyrmions Revealed by Spin-Polarized Scanning Tunneling Microscopy. *J. Phys.: Condens. Matter* **2014**, *26*, 394002–394015.
10. Sonntag, A.; Hermenau, J.; Krause, S.; Wiesendanger, R. Thermal Stability of an Interface-Stabilized Skyrmion Lattice. *Phys. Rev. Lett.* **2014**, *113*, 077202–077205.
11. Gsell, S.; Fischer, M.; Brescia, R.; Schreck, M.; Huber, P.; Bayer, F.; Stritzker, B.; Schlom, D. G. Reduction of Mosaic Spread Using Iridium Interlayers: A Route to Improved Oxide Heteroepitaxy on Silicon. *Appl. Phys. Lett.* **2007**, *91*, 061501–061503.
12. Gsell, S.; Fischer, M.; Schreck, M.; Stritzker, B. Epitaxial Films of Metals from the Platinum Group (Ir, Rh, Pt and Ru) on YSZ-Buffered Si(111). *J. Cryst. Growth* **2009**, *311*, 3731–3736.
13. Fischer, M.; Gsell, S.; Schreck, M.; Brescia, R.; Stritzker, B. Preparation of 4-Inch Ir/YSZ/Si(001) Substrates for the Large-Area Deposition of Single-Crystal Diamond. *Diamond Relat. Mater.* **2008**, *17*, 1035–1038.
14. von Bergmann, K.; Heinze, S.; Bode, M.; Bihlmayer, G.; Blügel, S.; Wiesendanger, R. Complex Magnetism of the Fe Monolayer on Ir(111). *New J. Phys.* **2007**, *9*, 396–414.
15. von Bergmann, K.; Heinze, S.; Bode, M.; Vedmedenko, E. Y.; Bihlmayer, G.; Blügel, S.; Wiesendanger, R. Observation of a Complex Nanoscale Magnetic Structure in a Hexagonal Fe Monolayer. *Phys. Rev. Lett.* **2006**, *96*, 167203–167206.
16. Zeller, P.; Dänhardt, S.; Gsell, S.; Schreck, M.; Wintterlin, J. Scalable Synthesis of Graphene on Single Crystal Ir(111) Films. *Surf. Sci.* **2012**, *606*, 1475–1480.
17. Wiesendanger, R. Spin Mapping at the Nanoscale and Atomic Scale. *Rev. Mod. Phys.* **2009**, *81*, 1495–1550.
18. Schlenhoff, A.; Krause, S.; Herzog, G.; Wiesendanger, R. Bulk Cr Tips with Full Spatial Magnetic Sensitivity for Spin-Polarized Scanning Tunneling Microscopy. *Appl. Phys. Lett.* **2010**, *97*, 083104–083106.
19. Bode, M.; Heinze, S.; Kubetzka, A.; Pietzsch, O.; Nie, X.; Bihlmayer, G.; Blügel, S.; Wiesendanger, R. Magnetization-Direction-Dependent Local Electronic Structure Probed by Scanning Tunneling Spectroscopy. *Phys. Rev. Lett.* **2002**, *89*, 237205–237208.
20. von Bergmann, K.; Menzel, M.; Serrate, D.; Yoshida, Y.; Schröder, S.; Ferriani, P.; Kubetzka, A.; Wiesendanger, R.;

Heinze, S. Tunneling Anisotropic Magnetoresistance on the Atomic Scale. *Phys. Rev. B* **2012**, *86*, 134422–134425.
21. Gsell, S.; Fischer, M.; Bauer, T.; Schreck, M.; Stritzker, B. Yttria-Stabilized Zirconia Films of Different Composition as Buffer Layers for the Deposition of Epitaxial Diamond/Ir Layers on Si(001). *Diamond Relat. Mater.* **2006**, *15*, 479–485.